chemistry proceedings

Proceeding Paper

Ionogels: Polimeric and Sol-Gel Silica Nanoscaffolds of Ionic Liquids as Smart Materials

Antía Santiago [1], Pablo Vallet [1], Juan José Parajó [1,*], María Villanueva [1], Óscar Cabeza [2], Luis Miguel Varela [1] and Josefa Salgado [1,*]

[1] NaFoMAT Research Group, Departments of Applied Physics and Particle Physics, Faculty of Physics, Campus Vida, Universidade de Santiago de Compostela, 15782 Santiago de Compostela (A Coruña), Spain; e-mail@e-mail.com (A.S.); e-mail@e-mail.com (P.V.); e-mail@e-mail.com (M.V.); e-mail@e-mail.com (L.M.V.)

[2] Mesturas Research Group, Department of Physics and Earth Sciences, University of A Coruña, A Coruña, Spain; e-mail@e-mail.com (Ó.C.)

* Correspondence: juanjose.parajo@usc.es (J.J.P.); j.salgado.carballo@usces (J.S.)

† Presented at the 26th International Electronic Conference on Synthetic Organic Chemistry; Available online: https://ecsoc-26.sciforum.net.

Abstract: The purpose of this work is to check the viability of mixtures of ionic liquids and lithium salt as electrolyte of Li- batteries. Firstly, the determination of the thermo-electrical properties of liquids mixtures of the ionic liquid N-butyl-N-methyl-pyrrolidinium bis(trifluoromethanesulfonyl)imide [BMPyrr][TFSI] with [Li][TFSI] salt at different concentrations was performed. Additionally, a comparison between these results with the corresponding to ionogels of these mixtures designed by two different gelation methods, one of them using Poly (vinylidene fluoride) (PVDF) as supporting matrix and the other one using a silica matrix.

Keywords: electrolyte; polymer; energy storage; ionic liquids

Citation: Santiago, A.; Vallet, P.; Parajó, J.J.; Villanueva, M.; Cabeza, Ó.; Varela, L.M.; Salgado, J. Ionogels: Polimeric and Sol-Gel Silica Nanoscaffolds of Ionic Liquids as Smart Materials. **2022**, *4*, x. https://doi.org/10.3390/xxxxx

Academic Editor(s): Julio A. Seijas

Published: 15 November 2022

1. Introduction

The energy transition towards forms of production and storage that allow complete sustainability and decarbonisation of the economic cycle is, at once, an urgent requirement of the current climate situation. The unstoppable energy transition process towards an increasingly sustainable and climate-neutral model, based on renewable energies, is related with an efficient storage and a sustainable consumption of this energy and it is a huge worldwide challenge involving the scientific community, politicians and all society [1].

With regards to the efficient energy storage, as a result of the development of 4th and 5th generation recyclable batteries, new materials are one of the critical topics in current studies, especially for electrolyte and electrode designs [2]. In latest years, research related to new electrochemical materials has experienced a great upgrade. One of the most promising materials are ionic liquids (ILs), which are organic salts formed by a cation and an anion whose melting point is below 100 °C. The tuneability of the properties of ILs from the infinity combinable anions and cations and the possibility of introducing functional groups in their alkyl chains, make these fluids appropriate for many industrial applications as for example, electrolytes in mixtures of ILs and inorganic salts, mainly lithium salts [3,4]

ILs confinement in a matrix improves handling while reducing the possibility of spillage and its grave consequences. This immobilization of ILs (or mixtures with inorganic salts) is known as gelation, and the resulting material is denominated ionogel or ionic gels.

In this work, a pure IL (1-Butyl-1-methylpyrrolidinium bis(trifluoromethylsulfonyl)imide) in liquid and gel state, obtained by two different routes, is analysed as a functional battery electrolyte in terms of broad band dielectric spectroscopy (BBDS). The effect of lithium salt addition to liquid and gel samples was also studied in terms of ionic conductivity.

2. Materials and Methods

2.1. Chemicals

For performing this work, an IL and a lithium salt with common anion, in liquid and gel form were selected. Table 1 shows a short description of the compounds used, molecular mass, short name, CAS identification number and provenance.

Table 1. Identification of Chemicals used in this work.

Name	Molecular Mass (g·mol^{-1})	Short Name	CAS Number	Purity Supplier
Ionic liquid: 1-butyl-1methyl-pyrrolidinium bis(trifluoromethanesulfonyl)imide	422.41	[BMPyrr][TFSI]	223437-11-4	>99 % IoLiTec
Salt: Lithium bis(trifluoromethanesulfonyl)imide	287.09	[Li][TFSI]	90076-65-6	>99 % Sigma Aldrich
Gel Precursor: Poly(vinylidene fluoride)	Mw ~ 534,000	PVDF	24937-79-9	Alfa Aesar
Gel Precursor: Tetramethyl orthosilicate	152.22	TMOS	681-84-5	98% Sigma Aldrich
Gel Precursor: Dimethoxydimethylsilane	120.22	DMDMS	1112-39-6	98% Sigma Aldrich

2.2. Gel Preparation

The first method is based on a solution of TMOS and DMDMS which in the presence of formic acid (FA) hydrolyses Si-O bonds forming a 3D network in whose pores the IL is immobilized. This gelation method was based on Brachet et al. [5] route, which can be summarized in three steps:

- Firstly, TMOS and DMDMS with a molar rate 0.65 to 0.35 are mixed and stirred during 10 min.
- Secondly, [BMPyrr][TFSI] in a 0.8 molar rate is added to the previous mixture and stirred 10 min more.
- Lastly, formic acid in a molar proportion of 3.3 is added, left in agitation during 2 min and finally introduced it in a Teflon mold.

The gel must remain covered for 2 days and another 5 days uncovered to achieve an accurate gelation. The gel may contain some impurities (precursors rest and other volatile products formed during the gelation), so a purifier vacuum process must be performed.

The second gelation method is based on PVDF, which is a nanometric powder which is mixed with dimethylformamide (DMF), whose only purpose is to triggers the gelation reaction [6]. The process followed to obtain the precursor matrix is:

- Mixing 8% PVDF in mass with 92% DMF and to stir during 3 h.
- Next, considering that PVDF is the hosting matrix (and DMF is only a solute to trigger the gelation process), the mass of PVDF vs IL is adjusted again, in mass proportions to 13% of PVDF and 87% of IL and is mixed during 3 min and kept in a Teflon mold.

The gel must remain covered for 2 days and open to environment for another 5 days, until the major part the DMF is evaporated. To finish the gelation process, the gel is under vacuum for 1 h, after, a heat treatment is performed, which consists of keeping the gel in vacuum at 110 °C during 40 min. When the heat treatment is completed, the gel must be under vacuum a minimum of 24 h to evaporate the impurities providing from gelation process.

2.3. Experimental Procedure

The electrical properties of the pure IL and mixtures have been analyzed through complex impedance spectroscopy in the frequency range of 20 Hz to 1 MHz and in the temperature interval of 273 K–323 K by using a RLC HP 4284A precision meter from Agilent, working with 8610 selectable frequencies between the selected frequency range. The basic accuracy of HP 4284 A is better than 0.05%. The applied sinusoidal voltage presents an amplitude of 0.2 V. This RLC precision meter presents 20 impedance parameters each one with its own measurement range, *i.e.*, G and B (conductance and susceptance, respectively) have a measurable range between 0.01 nS to 99.9999 S, while for Z′ and Z′′ (resistance and reactance, respectively) has a measure range between 0.01 mΩ to 99.9999 Ω.

A Swagelok coin cell with two parallel electrodes of stainless steel (4 mm radius and 1 mm of thickness) was used for experimental measurements. The short circuit compensation of the cell and its correction coefficient were considered to eliminate the effect of stray capacitance during the evaluation of the frequency dependent values of complex dielectric function [7].

A calibrated Julabo F25 thermostat was used to control the temperature of the sample; the uncertainty of the temperature was lower than 0.1 K. All the measurements were performed in an isothermal regime.

3. Results

The real dielectric constant ($\boldsymbol{\varepsilon}'$) spectra (Figure 1) differs in two characteristic regions in the studied frequency range, separated by a frequency around 2 kHz. At the low frequency range $\boldsymbol{\varepsilon}'$ decreases linearly over 5 magnitude orders with a slope greater than the unity as the frequency increases. The great response of $\boldsymbol{\varepsilon}'$ in low frequencies is due to electrode polarization contribution (EP). This effect represents the formation of the double electric layer (EDL) at the interface of the dielectric material and the electrode, due to the accumulation of ions and free charges [8].

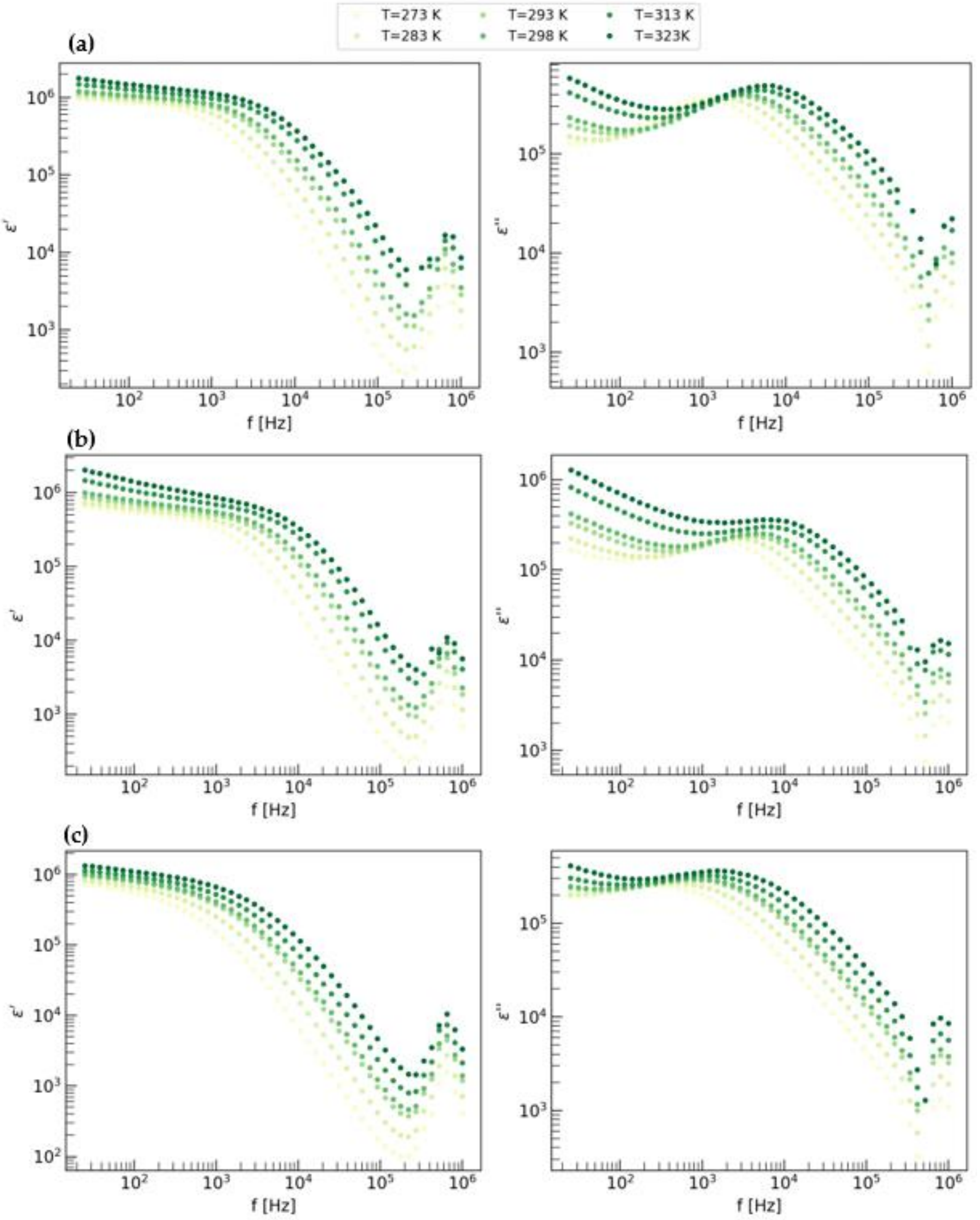

Figure 1. Real and Imaginary dielectric constant against frequency. (**a**) Pure [BMPyrr][TFSI]; (**b**)[BMPyrr][TFSI] PVDF gel. **(c)** [BMPyrr][TFSI] silica gel.

When the frequency increases the dipole rotational contribution becomes greater and $\boldsymbol{\varepsilon}'$ follows the Maxwell Boltzmann statistics [9]. As the frequency increases, the dielectric response decreased due to the difficulty of the ions to follow the electromagnetic vibrations. At a fixed frequency, the $\boldsymbol{\varepsilon}'$ response enlarges as the temperature increases which reveals that the concentration of the induced ions contributing to the formation of the EDL becomes greater with increasing temperature [10].

Regarding the imaginary part of dielectric constant ($\boldsymbol{\varepsilon}''$), it shows a plateau-like at low frequencies with a maximum that increases with temperature, followed by a linear decrement in a double-logarithmic scale. The decrement slope is approximately −1.00 which is characteristic to the ohmic region (the current density has a linear response with the applied electric field) [11]. The ohmic region varies as the increasing temperature since the initial frequency moves to greater frequencies. The plateau at low frequencies is caused by non-aligned lines of the ions and the applied electric field [12].

When temperature is over 40 °C the ohmic region of pure [BMPyrr][TFSI] is out of the studied region, so it is not possible to obtain the ionic conductivity by the applied method, becoming necessary to enlarge the frequency range over 1 MHz.

Every compound shows an increasing conductivity as increasing temperature (Figure 2). When temperature rise, the viscosity of the compound becomes lower, so the ions can flow easily giving greater transport properties.

The salt addition triggers a decrease in ionic conductivity due to a reduction in fluidity (increase of viscosity with salt addition). The descend in conductivity is due to the increasing formation of $\boldsymbol{Li(TFSI)_2^-}$ as a result of the Li ions coordination with $\boldsymbol{TFSI^-}$ anions [13].

The gelation provokes a diminished conductivity in every temperature and salt concentration. The decrement in ionic conductivity is caused by not only ion concentration reduction in gelation, but also by mobility decrement that could be due to the nanoconfinement in the matrix scaffold (Figure 2).

The silica gel ionic conductivity is lower than PVDF gel, becoming the half at 50 °C (Table 2). The reason is that on silica gels the IL proportion is much lower than PVDF gels (0.8 molar rate in silica gels, 83% mass in PVDF gels), that reduces ions proportion and the conductivity.

Both liquid and gel PVDF and silica samples follow a VFT behavior [14], that suggest that in both states is similar and the dynamic structural and the energy process of conduction does not vary substantially (Figure 2).

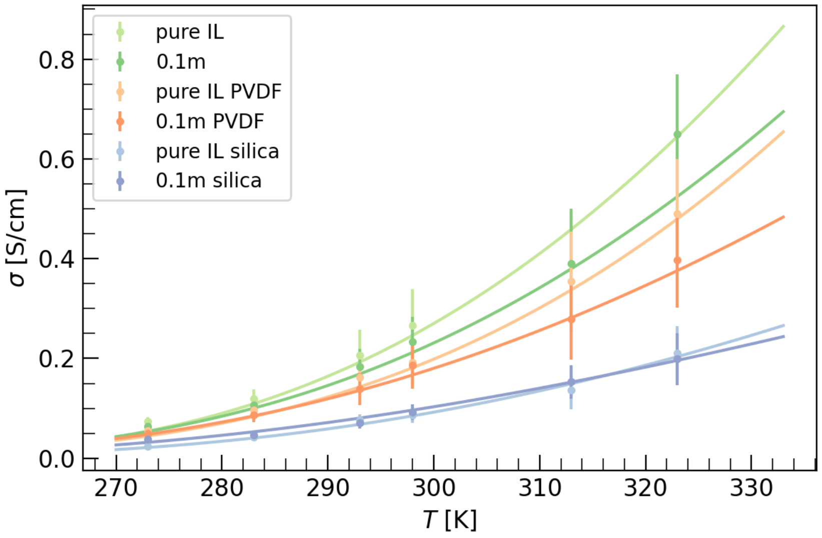

Figure 2. Ionic conductivity against temperature.

Table 2. Compound ionic conductivity at different temperatures.

T [°C]	Pure IL	0.1 m	Pure PVDF	0.1 m PVDF	Pure Silica	0.1 m Silica
0	0.0735(90)	0.0642(63)	0.0546(51)	0.0495(59)	0.0240(22)	0.0388(37)
10	0.0119(90)	0.106(13)	0.096(13)	0.086(13)	0.0425(51)	0.0473(53)
20	0.207(51)	0.183(36)	0.162(26)	0.139(32)	0.076(12)	0.071(11)
25	0.266(73)	0.233(51)	0.192(43)	0.186(47)	0.087(16)	0.092(16)
40		0.39(11)	0.355(99)	0.279(81)	0.137(39)	0.153(34)
50		0.65(12)	0.49(11)	0.397(95)	0.211(54)	0.199(52)

4. Conclusions

Impedance and dielectric properties of solution phase and gel of [BMPyrr][TFSI] have been studied in this work as well as the effect of the salt addition.

- The mobility of ions becomes greater when temperature increase.
- An enhancement on ionic conductivity is observed with temperature, that could be justified with a reduce on viscosity.
- Conductivity decreases with salt addition due to an increase on viscosity, and also decreases with the nanoconfinement of the IL in the matrix scaffolds, probably due to electrostatic interactions among IL and the nano-scaffold.

Author Contributions: Conceptualization, L.M.V., J.S. and J.J.P.; methodology, A.S., P.V. software, A.S. and P.V.; validation, A.S., P.V., J.J.P., M.V., Ó.C., L.M.V. and J.S.; data curation, A.S., P.V. and J.J.P.; writing—original draft preparation, A.S., P.V., J.J.P. and J.S.; writing—review and editing, A.S., P.V., J.J.P., M.V., Ó.C., L.M.V. and J.S.; supervision, J.J.P., M.V. and J.S.; project administration, Ó.C. and L.M.V.; funding acquisition, A.S., P.V., J.J.P., M.V., Ó.C., L.M.V. and J.S. All authors have read and agreed to the published version of the manuscript.

Funding: This work was supported by Spanish Ministry of Economy and Competitiveness and FEDER Program through the project MAT2017-89239-C2-1-P and the Network Ionic Systems for energy sustainability (SISE) RED2018-102679-T and by Xunta de Galicia through GRC ED431C 2020/10 project and the Galician Network of Ionic Liquids (ReGaLIs) ED431D 2017/06.

Institutional Review Board Statement: Not applicable.

Informed Consent Statement: Not applicable.

Data Availability Statement: Not applicable.

Acknowledgments: P. Vallet and J. J. Parajó thank funding support of FPI Program from Spanish Ministry of Science, Education and Universities and I2C postdoctoral Program of Xunta de Galicia, respectively.

Conflicts of Interest: The authors declare no conflict of interest.

References

1. Arbabzadeh, M.; Sioshansi, R.; Johnson, J.X.; Keoleian, G.A. The Role of Energy Storage in Deep Decarbonization of Electricity Production. *Nat. Commun.* **2019**, *10*, 3413. https://doi.org/10.1038/s41467-019-11161-5.
2. Menne, S.; Pires, J.; Anouti, M.; Balducci, A. Protic Ionic Liquids as Electrolytes for Lithium-Ion Batteries. *Electrochem. Commun* .**2013**, *31*, 39–41. https://doi.org/10.1016/j.elecom.2013.02.026.
3. Liew, C.W.; Ramesh, S.; Ramesh, K.; Arof, A.K. Preparation and Characterization of Lithium Ion Conducting Ionic Liquid-Based Biodegradable Corn Starch Polymer Electrolytes. *J. Solid State Electrochem.* **2012**, *16*, 1869–1875. https://doi.org/10.1007/s10008-012-1651-5.
4. Russina, O.; Caminiti, R.; Méndez-Morales, T.; Carrete, J.; Cabeza, O.; Gallego, L.J.; Varela, L.M.; Triolo, A. How Does Lithium Nitrate Dissolve in a Protic Ionic Liquid? *J. Mol. Liq.* **2015**, *205*, 16–21. https://doi.org/10.1016/j.molliq.2014.08.007.
5. Brachet, M.; Gaboriau, D.; Gentile, P.; Fantini, S.; Bidan, G.; Sadki, S.; Brousse, T.; le Bideau, J. Solder-Reflow Resistant Solid-State Micro-Supercapacitors Based on Ionogels. *J. Mater. Chem. A Mater.* **2016**, *4*, 11835–11843. https://doi.org/10.1039/c6ta03142k.
6. le Bideau, J.; Viau, L.; Vioux, A. Ionogels, Ionic Liquid Based Hybrid Materials. *Chem. Soc. Rev.* **2011**, *40*, 907–925. https://doi.org/10.1039/c0cs00059k.
7. Mehrotra, S.; Kumbharkhane, A.; Chaudhari, A. Theoretical and Experimental Aspects of Time Domain Permittivity Spectroscopy. In *Binary Polar Liquids*; Elsevier: Amsterdam, The Netherlands, 2017; pp. 1–43.
8. Vadhva, P.; Hu, J.; Johnson, M.J.; Stocker, R.; Braglia, M.; Brett, D.J.L.; Rettie, A.J.E. Electrochemical Impedance Spectroscopy for All-Solid-State Batteries: Theory, Methods and Future Outlook. *ChemElectroChem* **2021**, *8*, 1930–1947.
9. Rana, V.A.; Barot, D.K.; Vankar, H.P.; Pandit, T.R.; Karakthala, J.B. AC/DC Conductivity and Dielectric Relaxation Behavior of Ionic Solutions of 1-Butyl-3-Methylimidazolium Chloride in Methanol. *J. Mol. Liq.* **2019**, *296*, 111804. https://doi.org/10.1016/j.molliq.2019.111804.
10. *Broadband Dielectric Spectroscopy*; Kremer, F., Schönhals, A., Eds.; Springer Berlin Heidelberg: Berlin/Heidelberg, Germany, 2003; ISBN 978-3-642-62809-2.
11. Vallet, P.; Bouzón-Capelo, S.; Méndez-Morales, T.; Gómez-González, V.; Arosa, Y.; de la Fuente, R.; López-Lago, E.; Rodríguez, J.R.; Gallego, L.J.; Parajó, J.J.; et al. On the Physical Properties of Mixtures of Nitrate Salts and Protic Ionic Liquids. *J. Mol. Liq.* **2022**, *350*, 118483. https://doi.org/10.1016/j.molliq.2022.118483.
12. Tu, W.; Richert, R.; Adrjanowicz, K. Dynamics of Pyrrolidinium-Based Ionic Liquids under Confinement. I. Analysis of Dielectric Permittivity. *J. Phys. Chem. C* **2020**, *124*, 5389–5394. https://doi.org/10.1021/acs.jpcc.0c00156.
13. Kim, J.-K.; Lim, D.-H.; Scheers, J.; Pitawala, J.; Wilken, S.; Johansson, P.; Ahn, J.-H.; Matic, A.; Jacobsson, P. Properties of N-Butyl-N-Methyl-Pyrrolidinium Bis(Trifluoromethanesulfonyl) Imide Based Electrolytes as a Function of Lithium

Bis(Trifluoromethanesulfonyl) Imide Doping. *J. Korean Electrochem. Soc.* **2011**, *14*, 92–97. https://doi.org/10.5229/JKES.2011.14.2.092.

14. Noor, S.A.M.; Bayley, P.M.; Forsyth, M.; MacFarlane, D.R. Ionogels Based on Ionic Liquids as Potential Highly Conductive Solid State Electrolytes. *Electrochim. Acta* **2013**, *91*, 219–226. https://doi.org/10.1016/j.electacta.2012.11.113.